Langmuir Article

pubs.acs.org/Langmuir

pH-Induced Simultaneous Synthesis and Self-Assembly of 3D Layered β-FeOOH Nanorods

Xiao-Liang Fang, Yue Li, Cheng Chen, Qin Kuang,* Xiang-Zhi Gao, Zhao-Xiong Xie, Su-Yuan Xie,* Rong-Bin Huang, and Lan-Sun Zheng

State Key Laboratory for Physical Chemistry of Solid Surfaces and Department of Chemistry, College of Chemistry and Chemical Engineering, Xiamen University, Xiamen 361005, P. R. China

Received July 28, 2009. Revised Manuscript Received September 20, 2009

Higher-ordered architectures self-assembly of nanomaterials have recently attracted increasing attention. In this work, we report a spontaneous and efficient route to simultaneous synthesis and self-assembly of 3D layered β-FeOOH nanorods depending on a pH-induced strategy, in which the continuous change of pH is achieved by hydrolysis of $FeCl_3 \cdot 6H_2O$ in the presence of urea under hydrothermal conditions. The electron microscopy observations reveal that the square-prismic β-FeOOH nanorods are self-assembled in a side-by-side fashion to form highly oriented 2D nanorod arrays, and the 2D nanorod arrays are further stacked in a face-to-face fashion to form the final 3D layered architectures. On the basis of time-dependent experiments, a multistage reaction mechanism for the formation of the 3D layered β-FeOOH nanorods architecture is presented, involving the fast growth and synchronous self-assembly of the nanorods toward 1D, 2D, and 3D spontaneously. The experimental evidence further demonstrates that the urea-decomposition-dependent pH continuously changing in the solution, spontaneously altering the driving force competition between the electrostatic repulsive force and the attractive van der Waals force among the nanorods building blocks, is the essential factor to influence the self-assembly of the β-FeOOH nanorods from 1D to 3D.

1. Introduction

Self-assembly of discrete nanostructures into macroscopic higher-ordered architectures can create interesting models to investigate the chemical and physical interactions among the nanocrystals[1,2] and also offers new opportunities to fabricate functional materials and nanodevices.[3−10] Therefore, it has attracted increasing attention in both fundamental research and practical applications over the past years. In principle, the self-assembly of nanostructures strongly depends on the nanoparticle interactions,[11,12] the particle size distribution,[13] and the particle shape.[14,15] In comparison with the monodisperse spherical nanoparticles that usually form a fcc close-packing pattern, the polyhedral nanoparticles (e.g., rods, octahedra, and cubes) behaving as building blocks exhibit a variety of self-assembling fashions.[16−20] Nowadays, the prevalent self-assembly approaches include droplet evaporation,[21−24] mixing nonsolvent,[25,26] Langmuir−Blodgettry technique,[27−29] and small-molecule or polymer mediator-induced assembly.[30−33] In addition, as an important method for self-assembly, the surface template-assisted self-assembly approach based on the lithographically defined physical

*Corresponding authors: e-mail qkuang@xmu.edu.cn (Q.K.), syxie@xmu.edu.cn (S.-Y.X.); Fax +86-592-2183047; Tel +86-592-2185191.

(1) Kalsin, A. M.; Fialkowski, M.; Paszewski, M.; Smoukov, S. K.; Bishop, K. J. M.; Grzybowski, B. A. *Science* **2006**, *312*, 422.
(2) Shevchenko, E. V.; Talapin, D. V.; Kotov, N. A.; O'Brien, S.; Murray, C. B. *Nature* **2006**, *439*, 55.
(3) Fan, H. Y.; Yang, K.; Boye, D. M.; Sigmon, T.; Malloy, K. J.; Xu, H. F.; López, G. P.; Brinker, C. J. *Science* **2004**, *304*, 567.
(4) Xia, Y. N.; Gates, B.; Li, Z. Y. *Adv. Mater.* **2001**, *13*, 409.
(5) Lu, Y.; Yin, Y. D.; Xia, Y. N. *Adv. Mater.* **2001**, *13*, 415.
(6) Tao, A. R.; Ceperley, D. P.; Sinsermsuksakul, P.; Neureuther, A. R.; Yang, P. D. *Nano Lett.* **2008**, *8*, 4033.
(7) Lee, J. S.; Shevchenko, E. V.; Talapin, D. V. *J. Am. Chem. Soc.* **2008**, *130*, 9673.
(8) Shevchenko, E. V.; Ringler, M.; Schwemer, A.; Talapin, D. V.; Klar, T. A.; Rogach, A. L.; Feldmann, J.; Alivisatos, A. P. *J. Am. Chem. Soc.* **2008**, *130*, 3274.
(9) Ding, T.; Song, K.; Clays, K.; Tung, C. H. *Adv. Mater.* **2009**, *21*, 1936.
(10) Pietrobon, B.; McEachran, M.; Kitaev, V. *ACS Nano* **2009**, *3*, 21.
(11) Pileni, M. P. *J. Phys. Chem. B* **2001**, *105*, 3358.
(12) Whitesides, G. M.; Boncheva, M. *Proc. Natl. Acad. Sci. U.S.A.* **2002**, *99*, 4769.
(13) Rogach, A. L.; Talapin, D. V.; Shevchenko, E. V.; Kornowski, A.; Haase, M.; Weller, H. *Adv. Funct. Mater.* **2002**, *12*, 653.
(14) Jana, N. R. *Angew. Chem., Int. Ed.* **2004**, *43*, 1536.
(15) Song, Q.; Ding, Y.; Wang, Z. L.; Zhang, Z. J. *J. Phys. Chem. B* **2006**, *110*, 25547.
(16) Ghezelbash, A.; Koo, B.; Korgel, B. A. *Nano Lett.* **2006**, *6*, 1832.
(17) Carbone, L.; Nobile, C.; Giorgi, M. D.; Sala, F. D.; Morello, G.; Pompa, P.; Hytch, M.; Snoeck, E.; Fiore, A.; Franchini, I. R.; Nadasan, M.; Silvestre, A. F.; Chiodo, L.; Kudera, S.; Cingolani, R.; Krahne, R.; Manna, L. *Nano Lett.* **2007**, *7*, 2942.
(18) Lu, W. G.; Liu, Q. S.; Sun, Z. Y.; He, J. B.; Ezeolu, C.; Fang, J. Y. *J. Am. Chem. Soc.* **2008**, *130*, 6983.
(19) Zhang, J.; Kumbhar, A.; He, J. B.; Das, N. C.; Yang, K. K.; Wang, J. Q.; Wang, H.; Stokes, K. L.; Fang, J. Y. *J. Am. Chem. Soc.* **2008**, *130*, 15203.
(20) Chang, C. C.; Wu, H. L.; Kuo, C. H.; Huang, M. H. *Chem. Mater.* **2008**, *20*, 7570.
(21) Xu, J.; Xia, J. F.; Lin, Z. Q. *Angew. Chem., Int. Ed.* **2007**, *46*, 1860.
(22) Bigioni, T. P.; Lin, X. M.; Nguyen, T. T.; Corwin, E. I.; Witten, T. A.; Jaeger, H. M. *Nat. Mater.* **2006**, *5*, 265.
(23) Querner, C.; Fischbein, M. D.; Heiney, P. A.; Drndió, M. *Adv. Mater.* **2008**, *20*, 2308.
(24) Ming, T.; Kou, X. S.; Chen, H. J.; Wang, T.; Tam, H. L.; Cheah, K. W.; Chen, J. Y.; Wang, J. F. *Angew. Chem., Int. Ed.* **2008**, *47*, 9685.
(25) Shevchenko, E. V.; Talapin, D. V.; Rogach, A. L.; Kornowski, A.; Haase, M.; Weller, H. *J. Am. Chem. Soc.* **2002**, *124*, 11480.
(26) Shevchenko, E.; Talapin, D.; Kornowski, A.; Kötzler, J.; Haase, M.; Rogach, A. L.; Weller, H. *Adv. Mater.* **2002**, *14*, 287.
(27) Huang, J. X.; Kim, F.; Tao, A. R.; Connor, S.; Yang, P. D. *Nat. Mater.* **2005**, *4*, 896.
(28) Tao, A. R.; Sinsermsuksakul, P.; Yang, P. D. *Nat. Nanotechnol.* **2007**, *2*, 435.
(29) Tao, A. R.; Huang, J. X.; Yang, P. D. *Acc. Chem. Res.* **2008**, *41*, 1662.
(30) Fan, H. Y.; Leve, E.; Gabaldon, J.; Wright, A.; Haddad, R. E.; Brinker, C. J. *Adv. Mater.* **2005**, *17*, 2587.
(31) Bai, F.; Wang, D. S.; Huo, Z. Y.; Chen, W.; Liu, L. P.; Liang, X.; Chen, C.; Wang, X.; Peng, Q.; Li, Y. D. *Angew. Chem., Int. Ed.* **2007**, *46*, 6650.
(32) Zhuang, J. Q.; Wu, H. M.; Yang, Y. A.; Cao, Y. C. *Angew. Chem., Int. Ed.* **2008**, *47*, 2208.
(33) Park, S. Y.; Lytton-Jean, A. K. R.; Lee, B.; Weigand, S.; Schatz, G. C.; Mirkin, C. A. *Nature* **2008**, *451*, 553.

template[34] or self-organized chemical template[35] can directly achieve assembled pattern of building blocks on substrates, and thus it is often used in the investigation of self-assembly.[36,37] All of these methods above typically require to prefabricate tailor-made building blocks with uniform shape and size by means of specific synthetic routes or tedious size selection processes before the self-assembly. Consequently, simultaneous synthesis and self-assembly, by which the nascent building blocks can be spontaneously assembled during their growth process, are highly desirable.[38,39]

β-Ferric oxyhydroxide (β-FeOOH), a useful semiconductor with a band gap of 2.12 eV, is widely applied as pigment in commodity industry,[40] as catalysts in oxidation/reduction reactions and hydroprocessing of coal,[41] as positive electrode materials in lithium batteries,[42,43] and as raw materials for hard and soft magnets.[44,45] Over the recent decades, rod-shaped β-FeOOH has attracted intensive attentions as it is an ideal experimental model for investigating self-ordering behavior of colloidal nanorods in suspensions.[46−54] It has been found for a long time that uniform β-FeOOH nanorods facilitate to be obtained by slow hydrolysis of $FeCl_3$ and also to be spontaneously self-assembled to an ordered architecture (i.e., Schiller layers) with the iridescence color by long-time stewing or droplet evaporation.[46−54] In recent years, H. Maeda and Y. Maeda et al. have demonstrated by means of various optical and electron microscopy techniques that the Schiller layers originating from self-assembly of β-FeOOH nanorods are of the liquid crystal nature, and they consist of different phases, depending on the length/diameter ratio (L/W) of the nanorods as well as the initial density and pH of nanorod suspension (i.e., sols).[51−53] It should be in particular pointed out that, among these factors above, the pH plays a critical role in the stability of colloid suspensions, which may break the balance between interparticle electrostatic repulsive forces and van der Waals acttractive forces by changing surface charges of the particles.[53] Even the self-assembly mechanism of β-FeOOH nanorods has been appropriately discussed, development in the methodology to reach high-quality assembled materials of the β-FeOOH nanorods is relatively slow. Most of the present synthetic methods are very time-consuming, usually lasting for several months.[46−54] Therefore, designing a simple and effective self-assembly route is highly desirable from the viewpoint of fundamental research.

In this study, we propose a fast and facile one-step "bottom up" approach to simultaneously synthesize and self-assemble 3D layered square-prismic β-FeOOH nanorod arrays in the solution. In view of the absence of the surfactants or other external assistant effects, the proposed process is an ideal experimental model to investigate self-assembly of nonspherical nanoparticles with the only driving force of interparticle interaction. The competition between the electrostatic repulsive force and attractive van der Waals force among the building blocks, tunable by the urea-decomposition-dependent pH of the solution, is revealed to be essential for constructing desired β-FeOOH nanorods structures from 1D to 3D.

2. Experimental Section

Synthesis of 3D Layered Self-Assembled β-FeOOH Nanorods Based on the pH-Induced Strategy. Ferric chloride ($FeCl_3 \cdot 6H_2O$) and urea were purchased from Sinopharm Chemical Reagent Co. (Shanghai, China). All reagents are of analytical grade and used without further purification. In a typical experiment, $FeCl_3 \cdot 6H_2O$ (270 mg, 1 mmol) and urea (120 mg, 2 mmol) were added into deionized water (16 mL) and stirred for several minutes until an orange transparent solution was obtained. The solution was then transferred into a 20 mL Teflon-lined stainless steel autoclave. The sealed autoclave was warmed up at a rate of 1.5 °C min^{-1} to 120 °C and then maintained for 10 h. Finally, the autoclave was naturally cooled to room temperature. The brown precipitation was collected by centrifugation and washed with deionized water for three times. To investigate the role of urea, in addition, a urea-free control experiment was further carried out under the same reaction conditions.

Synthesis of Self-Assembled β-FeOOH Nanorods Based on the Droplet Evaporation Strategy. The synthetic procedure of monodisperse building blocks (i.e., spindlelike β-FeOOH nanorods) is similar to the synthesis procedure for the 3D layered self-assembled β-FeOOH nanorods mentioned above, but in the absence of urea and changing the reaction time from 10 to 1 h. After reaction, the spindlelike β-FeOOH nanorods were collected by centrifugation, washed with deionized water for three times, and then redispersed into deionized water (0.25 mL). For the preparation of β-FeOOH nanorod assemblies, a drop (about 10 μL) of well-dispersed suspension of β-FeOOH nanorods was dropped onto a clean silicon substrate in a culture dishes with a cap. Kept at room temperature over 6 h for water evaporation, ringlike self-assembled β-FeOOH nanorods were obtained on the silicon substrate.

Characterization of the Samples. The phase of the products was characterized by X-ray powder diffraction (XRD, Panalytical X'pert PRO diffractometer with Cu Kα radiation). The morphologies of the products were observed by scanning electron microscopy (SEM, Hitachi S-4800 and LEO 1530). The internal structures of the samples were characterized by high-resolution transmission electron microscopy (HRTEM, TECNAI F-30 with an accelerating voltage of 300 kV). The pore size distribution plot of the products was measured by Barrett−Joyner−Halenda (BJH) method on a Micrometrics ASAP 2020 system. The zeta potential and size distribution measurements were performed on Nano-ZS&MPT-2 (Malvern), and the pH of the solution was recorded with pH meter S20 (Mettler Toledo).

3. Results and Discussion

The pH-induced simultaneous synthesis and self-assembly of 3D β-FeOOH nanorods was carried out through a hydrothermal route at 120 °C by using $FeCl_3 \cdot 6H_2O$ and urea as raw materials. Designing of such a reaction system involving $FeCl_3$ and urea is based on the following reasons. First, $FeCl_3$ facilitates to hydrolyze in weakly acidic, neutral, or basic aqueous solutions for synthesis of β-FeOOH nanorods.[46−54] Second, urea can slowly

(34) Lee, I.; Zheng, H. P.; Rubner, M. F.; Hammond, P. T. *Adv. Mater.* **2002**, *14*, 572.
(35) Choi, J. H.; Adams, S. M.; Ragan, R. *Nanotechnology* **2009**, *20*, 065301.
(36) Hammond, P. T. *Adv. Mater.* **2004**, *16*, 1271.
(37) Smith, R. K.; Lewis, P. A.; Weiss, P. S. *Prog. Surf. Sci.* **2004**, *75*, 1.
(38) Soulantica, K.; Maisonnat, A.; Fromen, M. C.; Casanove, M. J.; Chaudret, B. *Angew. Chem., Int. Ed.* **2003**, *42*, 1945.
(39) Wang, N.; Guo, L.; He, L.; Cao, X.; Chen, C. P.; Wang, R. M.; Yang, S. H. *Small* **2007**, *3*, 606.
(40) Ceus, J. W. E.; Tacobus, J. M. *Chem. Abstr.* **1973**, *78*, 32167m.
(41) Cornell, R. M.; Schwertmann, U. *The Iron Oxide. Structure, properties, Reactions, Occurrence and Uses*; VCH: Weinheim, 1996.
(42) Wang, X.; Chen, X. Y.; Gao, L. S.; Zheng, H. G.; Ji, M. R.; Tang, C. M.; Shen, T.; Zhang, Z. D. *J. Mater. Chem.* **2004**, *14*, 905.
(43) Xiong, Y. J.; Xie, Y.; Chen, S. W.; Li, Z. Q. *Chem.—Eur. J.* **2003**, *9*, 4991.
(44) Piao, Y. Z.; Kim, J. Y.; Na, H. B.; Kim, D. Y.; Beak, J. S.; Ko, M. K.; Lee, J. H.; Shokouhimehr, M.; Hyeon, T. *Nat. Mater.* **2008**, *7*, 242.
(45) Xiong, Y. J.; Li, Z. Q.; Li, X. X.; Hu, B.; Xie, Y. *Inorg. Chem.* **2004**, *43*, 6540.
(46) Zocher, H. *Z. Anorg. Allg. Chem.* **1925**, *147*, 91.
(47) Zocher, H.; Heller, W. *Z. Anorg. Allg. Chem.* **1930**, *186*, 75.
(48) Heller, W. *Comptes Rendus* **1935**, *201*, 831.
(49) Maeda, Y.; Hachisu, S. *Colloids Surf.* **1983**, *6*, 1.
(50) Maeda, Y.; Hachisu, S. *Colloids Surf.* **1983**, *7*, 357.
(51) Maeda, H.; Maeda, Y. *Langmuir* **1996**, *12*, 1466.
(52) Maeda, H.; Maeda, Y. *Nano Lett.* **2002**, *2*, 1073.
(53) Maeda, H.; Maeda, Y. *Phys. Rev. Lett.* **2003**, *90*, 018303.
(54) Farrell, D.; Dennis, C. L.; Lim, J. K.; Majeticha, S. A. *J. Colloid Interface Sci.* **2009**, *331*, 394.

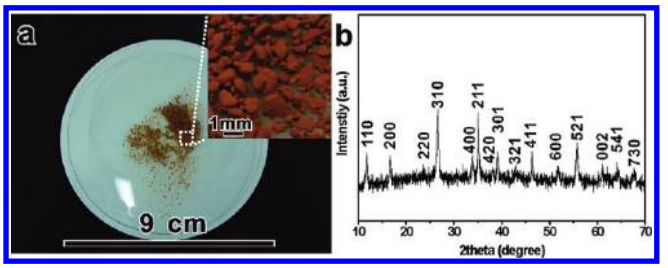

Figure 1. (a) Photo of the as-obtained products in a plate. Inset of (a): corresponding high-magnification photo. (b) XRD pattern of the as-obtained products.

decompose under hydrothermal conditions and thus act as a steady OH^- source which leads to a consistent change of the pH in the reaction solution. Third, an appropriate reaction temperature (i.e., 120 °C), which is required to obviously accelerate the hydrolysis of $FeCl_3$ and meanwhile ensure gently decomposing of urea, contributes to the fast formation of β-FeOOH nanorods taking precedence of the pH change. And finally, likely the most important, previous studies have demonstrated that the stability of colloid suspensions depends on the balance between the attractive van der Waals forces and the electrostatic repulsive forces,[55,56] which can be tuned by varying the pH of the solution. Details of the results and discussion regarding spontaneous formation of the 3D layered self-assembled β-FeOOH nanorods are elaborated as follows.

Figure 1a shows that the brown precipitation collected after the hydrothermal reaction contains some macroscopical solids. The XRD characterization (Figure 1b) indicates that the precipitation belongs to a tetragonal phase of β-FeOOH (JCPDS No. 34-1266).

A typical SEM image of the macroscopical solids is shown in Figure 2a, and its corresponding local enlargement (Figure 2a and the inset) reveals that the as-obtained macroscopic solids are constructed by 3D multilayered substructures. The typical high-magnification SEM image of a broken region (Figure 2b) indicates that every individual layer is composed of vertically standing self-assembled square-prismic nanorods with round ends, which are of ~200 nm in length and of 40−50 nm in width. More detailed morphological characteristic of the 3D self-assembled multilayered structures are shown in Figures S1 and S2 (Supporting Information). A typical self-assembled architecture composed of three flat layers is selected to be further investigated on the self-assembled fashion of the building blocks in detail (Figure 2c−f). The high-magnification SEM images (Figure 2d,e) recorded from two different regions (marked with *d* and *e* in Figure 2c) in the same layer (layer 3) reveal that all the square-prismic nanorods in the same layer are self-assembled by side-by-side attachment along the same orientations (as the solid arrows pointing to). The slight misalignment should be caused by the unbalanced size distribution of the nanorods. It should be pointed out that it is random for the packing between the adjacent layers where the square-prismic nanorods are aligned along different orientations (as marked with the solid and dashed arrows in Figure 2f).

The more detailed structural information on the as-synthesized self-assembled nanorods was further provided by TEM. Figure 3a shows a TEM image of a single layer of self-assembled nanorods with a square-ordered pattern. The corresponding selected area electron diffraction (SAED) pattern taken along the *c* zone axis is analogously single-crystalline, indicating the highly oriented

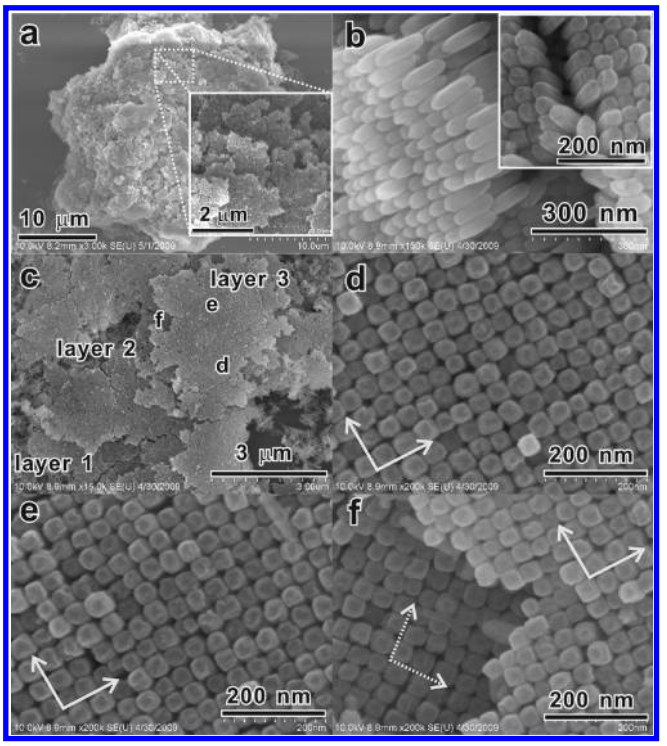

Figure 2. SEM characterization of the as-obtained 3D layered self-assembled β-FeOOH nanorods: (a) Typical solid with tens of micrometers in size. Inset: high-magnification image corresponding to the dashed region. (b) Typical broken region (side view). Inset: vertical view. (c) Typical fragment composed of three layers. Marks: regions *e* and *f* are corresponding to the regions observed in (d)−(f). (d, e) Self-assembled nanorods in the same layer. (f) Self-assembled nanorods in the adjacent two layers.

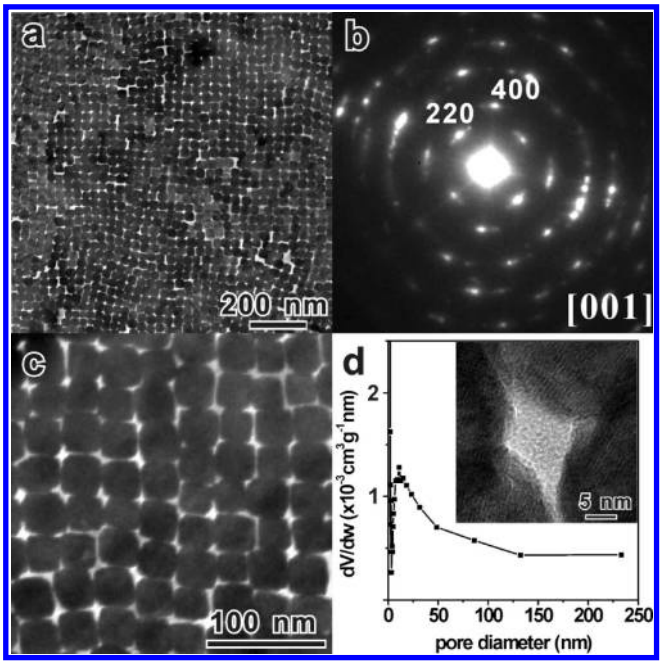

Figure 3. TEM characterization of a single layer as-synthesized self-assembled β-FeOOH nanorods: (a) low-magnification TEM image, (b) corresponding SAED pattern, and (c) high-magnification TEM image. (d) Pore size distribution curve of the as-obtained self-assembled β-FeOOH nanorods. Inset: typical TEM image of the channel.

(55) Derjaguin, B. V.; Landau, L. D. *Acta Physicochim. URSS* **1941**, *14*, 633.
(56) Verwey, E. J. W.; Overveek, J. T .G. *Theory of the Stability of Lyotropic Colloids*; Elsevier: Dover reprint, 2001.

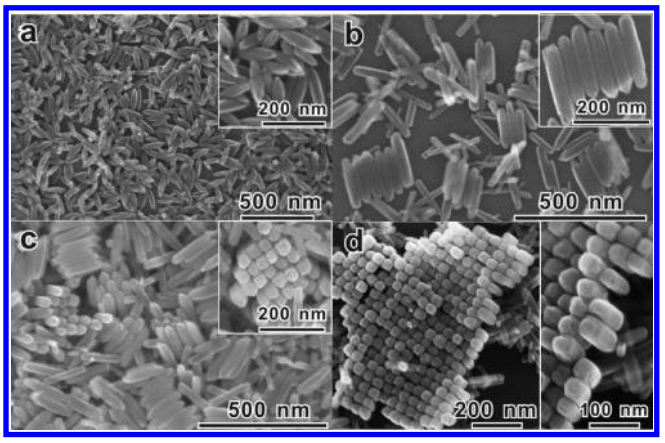

Figure 4. SEM images of the morphological evolution in the time-dependent experiments: (a) 1, (b) 3, (c) 5, and (d) 7 h (the insets: typical high-magnification images).

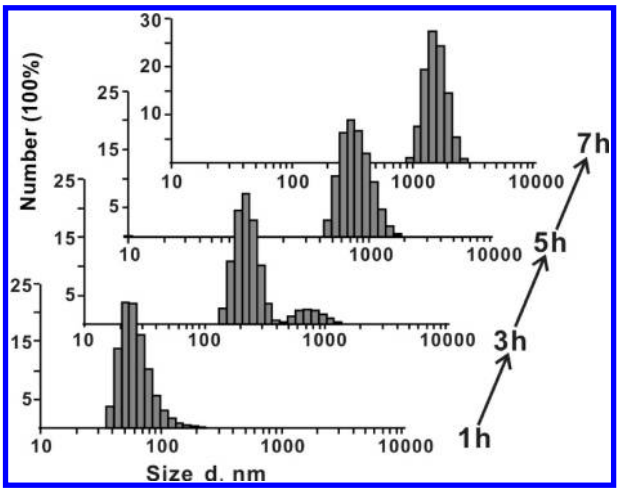

Figure 5. Size distribution evolution of the products obtained in the time-dependent experiments.

alignment of nanorods along both *a*- and *b*-axis. The diffraction spots are widened into narrow arcs due to the existence of misalignments among the building blocks. In addition, many vertical channels of 10 nm in average diameter are observed between adjacent incompact nanorods in the self-assembled layered structure (Figure 3c). The pore distribution diagram (Figure 3d) based on the BJH method further displays that the as-prepared product possesses a broad mesopore distribution around 11 nm, well consistent with the TEM observation (inset of Figure 3d).

To understand the simultaneous synthesis and self-assembly process, a series of time-dependent synthetic experiments are carried out, and the intermediate products obtained at different time intervals are further investigated by SEM for tracking morphological evolution (Figure 4). As shown in Figure 4a, the products obtained at 1 h are composed of monodisperse spindle-like nanorods of 50 nm in diameter and 180 nm in length. After reaction for 3 h, the products evolve to square-prismic nanorods, and correspondingly their diameters and lengths slightly increase (Figure 4b). Interestingly, some quantities of nascent square-prismic nanorods are found to aggregate side-by-side into some raftlike structures. When prolonging reaction time to 5 h, bundle-like nanorod assemblies of around hundreds of nanometers in size are dominant in the products (Figure 4c). At this stage, the self-assembled fashion of the β-FeOOH nanorods evolves from the 1D mode (i.e., the raftlike structure) to the 2D mode (i.e., the bundlelike structure). After reaction for 7 h, the rudiment of 3D self-assemblies, the layered self-assembled β-FeOOH nanorods of up to micrometer scale size are formed (Figure 4d). The whole morphological evolution reveals that the formation of the 3D self-assembled β-FeOOH nanorods undergoes a typical "bottom-up" pathway, which involves a fast nucleation and growth of building blocks followed by their 1D, 2D, and 3D self-assembly step by step.

To monitor the real self-assembling behavior of the β-FeOOH nanorods, the dynamic light scattering (DLS) technique that can *in situ* provide the size distributions of the intermediate products in the solution is further applied (Figure 5). After reaction for 1 h, the hydrodynamic diameters of the intermediate products possess a single size distribution with the peak value of 60−70 nm, which reveals that the spindlelike intermediates as primary particles are well dispersed in the solution at this reaction stage. After reaction for 3 h, the hydrodynamic diameter of the intermediates presents a mixture of size distribution, implying the existence of two distinct diffusing species in the solution. The primary distribution in the small size range should result from the dispersive primary particles (i.e., the square-prismic nanorods), and the minor distribution with the peak value of about 500 nm should be due to the appearance of some small self-assemblies (i.e., the raftlike arranged square-prismic nanorods). When the reaction lasts to 5 h, there is only a single distribution with a peak value of 700 nm in the large size range detected by DSL. This means that all the building blocks are self-assembled into the large aggregates at this stage. With the prolonging of reaction time, the hydrodynamic diameters of the products increase to a micrometer scale at reaction time of 7 h. Such a time-dependent size distribution evolution agrees well with the SEM observation shown in Figure 4. As a result, it can be concluded that the formation of 3D self-assembled β-FeOOH nanorods is indeed multistage and takes a synchronous synthesis and self-assembly process from the β-FeOOH nanorods building blocks spontaneously.

As is well-known, the stability of colloid suspensions depends on the balance between the electrostatic repulsive forces and attractive van der Waals forces.[55,56] In order to investigate the interparticle interactions, the pH of the reaction solution and zeta potential of the intermediate products are further detected during the reaction (Figure 6). At the early stage, the pH of the reaction system is acid (e.g., pH = 0.98 for 1 h). With the reaction proceeding, the pH gradually rose and finally is maintained at about 7 (Figure 6a, the curve of hollow dots). But, in contrast, the zeta potential of the intermediate products first increased and then gradually decreased to the isoelectric point (Figure 6a, the curve of solid dots). In principle, the zeta potential reflects the effective charge on the particles. It thus can be a probe to evaluate the amount of surface charge of the as-prepared β-FeOOH nanorods and the electrostatic repulsion between them. Obviously, the surface charge of the products has a close relation with the pH of the reaction system.

As we have designed, the pH change of the reaction system is the essential factor for inducing self-assemble behavior of the β-FeOOH nanorods, which results from slow decomposition of urea under the hydrothermal conditions. As shown in the urea-free control experiment (Figure 6b), no self-assembled nanorods are observed after the same reaction. Interestingly, the intermediate products obtained after reaction for 1 h are already monodisperse β-FeOOH nanorods, and the pH of the solution is always maintained at about 1 during the reaction (e.g., the pH after reaction for 1 and 10 h is equal to 1.06 and 0.97, respectively). So, in our synthetic methods, urea actually acts as a steady OH^- supply

through slowly decomposing. It should be pointed out that the change speed of pH is also crucial for the self-assembly process of the β-FeOOH nanorods. Take the sols of the spindlelike β-FeOOH nanorods as an example, the transparent sols flocculated into the loose sediment at the bottom of the solution if rapidly raising the pH from 1 to near neutral by adding alkaline solution (Figure 6c). SEM observation indicates that this sediment is composed of randomly agglomerated nanospindles (Figure 6d,e). So it can be concluded that the spontaneous formation of 3D self-assembled β-FeOOH nanorods is induced by the pH of the reaction system.

On the basis of the above experimental results, we propose four major steps in the formation of the 3D self-assembled β-FeOOH nanorods as follows: (i) formation of the building blocks; (ii) 1D self-assembly of the building blocks; (iii) 2D self-assembly of the building blocks; and (iv) 3D self-assembly of 2D self-assembled building blocks. This formation mechanism can be schematically depicted in Scheme 1.

In the step i, the building blocks, i.e., the β-FeOOH nanorods is formed through the hydrolysis reaction of Fe^{3+} ions as follows:

$$Fe^{3+} + 3H_2O \rightarrow Fe(OH)_3 + 3H^+ \quad (1)$$

$$Fe(OH)_3 \rightarrow FeO(OH) + H_2O \quad (2)$$

These β-FeOOH nanorods with high positive surface charges are well dispersive at this stage owing to the electrostatic repulsive force exceeding attractive van der Waals force between the building blocks. At the same time, the pH of reaction system begins to rises due to the decomposition reaction of urea as follows:

$$(NH_2)_2CO + H_2O \rightarrow 2NH_3 + CO_2 \quad (3)$$

$$NH_3 + H_2O \rightarrow NH_4^+ + OH^- \quad (4)$$

The formed OH^- ions can neutralize the positive surface charge of the β-FeOOH nanorods, leading to the change of the surface charge. With the decrease of the surface charge, the interparticle interactions gradually evolve from repulsive to attractive, and the dispersive square-prismic β-FeOOH nanorods tends to be self-assembled with each other to reduce the surface energy. As depicted in the step ii of Scheme 1, these freestanding β-FeOOH nanorods first form the 1D raftlike self-assemblies in the solution because the side-by-side assembling mode is energetically more favorable than the end-to-end assembling mode. To further reduce the surface energy, the raftlike self-assemblies will continuously attract those nearby freestanding nanorods or raftlike self-assemblies and assemble with them in the tetragonal-like packing mode. At this stage (i.e., step iii), the assembling of the β-FeOOH nanorods evolves from 1D to 2D. With the increase of the pH to near neutral, the electrostatic repulsive force between self-assemblies is negligible. Finally, some layers of adjacent square self-assembled nanorod arrays tend to be stacked up with each other and form a layered 3D architecture under the attractive van der Waals force, as shown in step iv. From the above presented mechanism, it can be found that the speed for pH changing in the reaction system is the key to achieve 3D self-assembly of β-FeOOH nanorods, which requires an appropriate dosage of urea in the synthetic procedure. In addition, because the self-assembly of the β-FeOOH nanorods take place simultaneously accompanying with the formation of nanorods in a closed reaction vessel, our proposed synthetic route is tolerant of external influence, such as environmental temperature and humidity.

According to the above discussion, the competition of the interparticle interactions (i.e., the electrostatic repulsive forces and attractive van der Waals force in the building blocks) is the

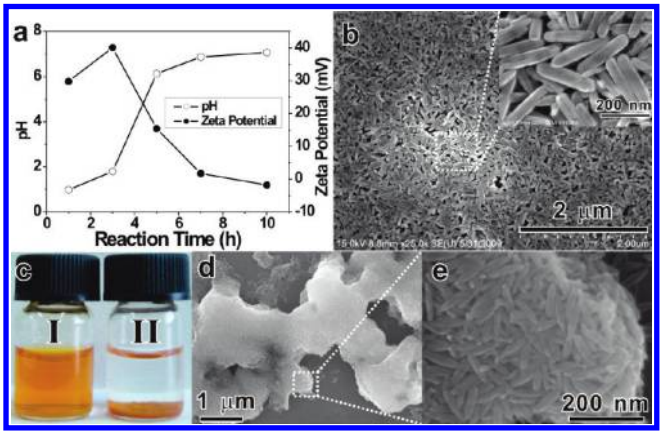

Figure 6. (a) pH of the reaction system (hollow dots) and the zeta potential of the intermediate products (solid dots) evolution in the time-dependent experiments. (b) SEM image of the products obtained after reaction for 10 h in the urea-free control experiment. Inset: corresponding high-magnification SEM image. (c) The photos to illustrate the flocculation of the stable nanospindle sols driven by adding alkaline solution. Marks: (I) the nanospindle sols, pH = 1; (II) the sediment, pH = 7. (d) Low-magnification SEM image and (e) corresponding high-magnification SEM image of the flocculation.

Scheme 1. Schematic Illustration for the Formation of the 3D Self-Assembled β-FeOOH Nanorods

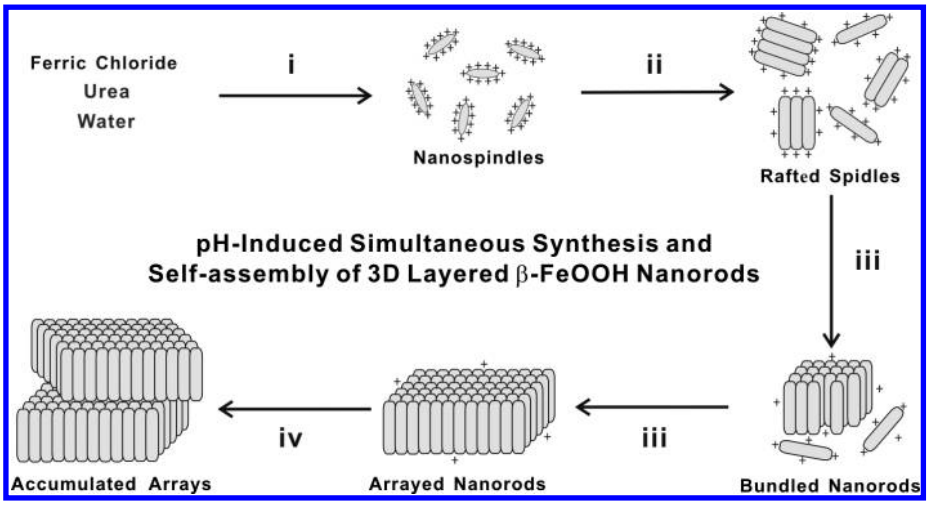

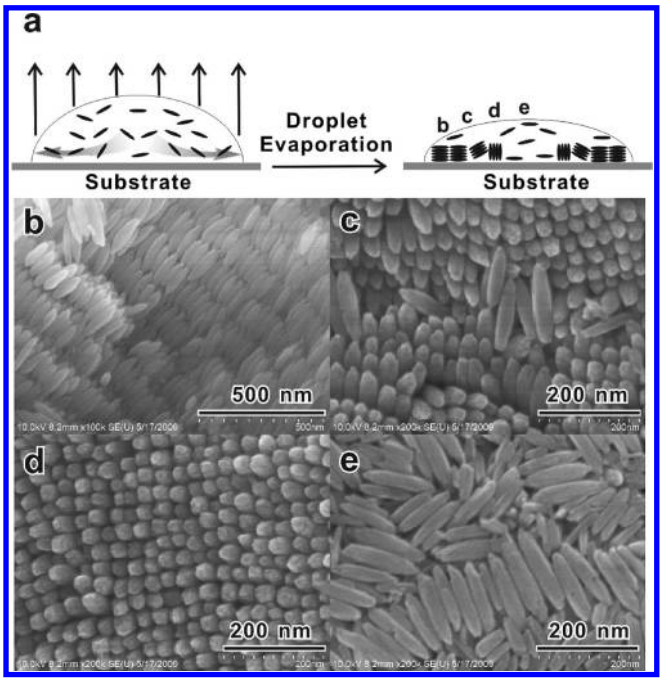

Figure 7. Self-assembly of monodisperse spindlelike β-FeOOH nanorods through a droplet evaporation route. (a) Schematic illustration for the droplet-evaporation-induced formation of self-assembled β-FeOOH nanorods. Marks: $b-e$ (from the edge to the center) correspond to the regions observed in (b)−(e). Four typical self-assembling fashions of the β-FeOOH nanorods observed from the $b-e$ regions: (b) nematic phase, (c) a mixture of nematic phase and smectic-A phase, (d) smectic-A phase, (e) disordered aggregation.

direct driving forces for self-assembly of the colloidal β-FeOOH nanorods, which can be tuned by the continuous pH change of the reaction system. Compared with the previously reported droplet evaporation,[24,52] such a self-assembling strategy is more simple and time-saving and facilitates the formation of nanostructures with high quality. In the droplet evaporation (schematically depicted in Figure 7a), apart from the interparticle interactions, both evaporation speed and various interfacial (e.g., solution−substrate, solution−gas, and solution−substrate−gas) forces also can greatly influence the self-assembling behavior of colloidal nanoparticles. The self-assembling behavior of colloidal nanoparticles is therefore more complex and uncontrollable in the synthetic systems of solution evaporation. The additional experiment provides the evidence that the self-assembled patterns of the β-FeOOH nanorods in different regions are dissimilar. The nematic phase is dominant in the region *b* (i.e., the edge of the droplet) where closely packed chains of the β-FeOOH nanorods through the end-to-end self-assembly are lying on the substrate (Figure 7b). In the region *d* neighboring to the center of the droplet, however, the main assembled pattern is the smectic-A phase where the standing upright β-FeOOH nanorods are side-by-side self-assembled together to form 2D nanorod arrays on the substrate and finally to a 3D layered architecture (Figure 7d). In addition to these uniform liquid phases, there are some disordered aggregated patterns in region *c* (i.e., the center of the droplet) and region *d* (i.e., the neighborhood of the edge of the droplet), as shown in parts c and e of Figure 7, respectively.

4. Conclusion

In summary, we have developed an effectual route to fabricate 3D layered self-assembled β-FeOOH nanorods based on a pH-induced strategy. Urea is critical in the proposed method, which can continuously change the pH of the reaction system, tune the interparticle interaction, and further induce the spontaneous self-assembly of the colloidal β-FeOOH nanorods through its slow decomposition. Despite that it is very simple and straightforward, the proposed simultaneous synthesis and self-assembly method is remarkably effective and reproducible to obtain high-quality 2D and 3D structures of nanorods building blocks. We believe that the present strategy will be very useful for the fundamental research and practical application on the self-assembled β-FeOOH nanorods and meanwhile provides an alternative pathway to assemble 3D structural analogues of other functional nanoparticles.

Acknowledgment. This work was supported financially by the NSFC (Grants 20525103, 20801045, 20531050, and 20725310) and the 973 Program (Grant 2007CB815301).

Supporting Information Available: Low-magnification SEM image of 3D self-assembled nanorods (Figure S1); detailed SEM characterization of the selected regions in Figure S1 (Figure S2). This material is available free of charge via the Internet at http://pubs.acs.org.